

FAR ULTRAVIOLET SPECTROSCOPIC EXPLORER SNAP-SHOT SURVEY OF O VI
VARIABILITY IN THE WINDS OF 66 OB-TYPE STARS

N. LEHNER,^{1,2} A. W. FULLERTON,^{1,3} D. MASSA,⁴ K. R. SEMBACH,⁵ AND J. ZSARGÓ¹

Version November 8, 2018

ABSTRACT

We have used the *Far Ultraviolet Spectroscopic Explorer (FUSE)* to conduct a snap-shot survey of O VI variability in the winds of 66 OB-type stars in the Galaxy and the Magellanic Clouds. These time series consist of two or three observations separated by intervals ranging from a few days to several months. Although these time series provide the bare minimum of information required to detect variations, this survey demonstrates that the O VI doublet in the winds of OB-type stars is variable on various scales both in time and velocity. For spectral types from O3 to B1, 64% vary in time. At spectral types later than B1, no wind variability is observed. In view of the limitations of this survey, this fraction represents a lower limit on the true incidence of variability in the O VI wind lines, which is very common and probably ubiquitous. In contrast, for S IV and P V, only a small percentage of the whole sample shows wind variations, although this may be principally due to selection effects. The observed variations extend over several hundreds of km s^{-1} of the wind profile and can be strong. The width over which the wind O VI profile varies is only weakly correlated with the terminal velocity (v_∞), but a significant correlation (close to a 1:1 relationship) is derived between the maximum velocity of the variation and v_∞ . High velocity O VI wind absorption features (possibly related to the discrete absorption components seen in other wind lines) are also observed in 46% of the cases for spectral types from O3 to B0.5. These features are variable, but the nature of their propagation cannot be determined from this survey. If X-rays can produce sufficient O VI by Auger ionization of O IV, and the X-rays originate from strong shocks in the wind, this study suggests that stronger shocks occur more frequently near v_∞ , causing an enhancement of O VI near v_∞ .

Subject headings: line: profiles – stars: winds – stars: mass-loss – stars: early-type

1. INTRODUCTION

The detection of wind profiles in the O VI $\lambda\lambda 1032, 1038$ resonance doublet in *Copernicus* spectra of stars with spectral types between O4 and B1 (Snow & Morton 1976; Morton 1979) provided the first evidence for the existence of high-energy, non-radiative processes in the outflows from hot stars. The presence of this ion was surprising, since only the hottest O stars are expected to produce it directly through photoionization. In a pivotal paper, Cassinelli & Olson (1979) demonstrated that X-rays can produce sufficient O VI by Auger ionization of O IV, which is the dominant ionization stage of oxygen in the winds of stars in the temperature range where O VI is observed. The X-ray flux required by the Auger mechanism was subsequently detected in spectra of OB-type stars obtained by the *Einstein* observatory (Harnden et al. 1979; Seward et al. 1979). Since the existence of O VI is linked directly to the presence of X-rays, the shape and strength of the O VI lines can be used to trace the distribution of hot, X-ray emitting gas in the winds of early-type stars (MacFarlane et al. 1993).

X-rays are believed to be caused by the formation of strong shocks in the wind, which convert mechanical energy of the flow into localized sources of heat. These shocks could arise from various processes, such as: (a)

the “line de-shadowing instability” intrinsic to the line-driving mechanism responsible for hot-star winds (Owocki et al. 1988); (b) the interfaces of large-scale co-rotating interactions regions (CIRs), which might be responsible for recurrent variability in hot-star winds (Mullan 1984; Cranmer & Owocki 1996); or (c) collisions (channeling) of material along closed (open) magnetic fields emanating from the surface of the star (ud Doula & Owocki 2002). Since these mechanisms involve the evolution of complicated, non-stationary flows, their tracers might be expected to exhibit substantial variations. For example, if the bulk of the X-rays or O VI ions are produced by a few strong shocks (as in the case of CIRs and simple magnetic field configurations), large variations might be expected as the distribution or strength of the shocks evolves. Conversely, little or no variability would be expected if the global distribution of the shocks (e.g., resulting from many ensembles of shocks generated by the line-deshadowing instability) do not change much with time. In either case, fluctuations in the tracers of the high energy processes provide information about the origin and distribution of the hottest gas in these outflows.

Until recently, X-rays were the predominant tracers of shock phenomena in the winds of hot stars. The limited X-ray data available suggest little short-term variability,

¹ Department of Physics and Astronomy, The Johns Hopkins University, 3400 N. Charles Street, Baltimore, MD 21218.

² Present address: Department of Astronomy, University of Wisconsin, 475 North Charter Street, Madison, WI 53706. nl@astro.wisc.edu

³ Department of Physics and Astronomy, University of Victoria, P.O. Box 3055, Victoria, BC V8W 3P6, Canada.

⁴ SGT Inc., NASA’s Goddard Space Flight Center, Code 681, Greenbelt, MD 20771.

⁵ Space Telescope Science Institute, 3700, San Martin Drive, Baltimore, MD 21218

which is generally interpreted as implying that many shock ensembles are present in the wind (see, e.g., Feldmeier, Puls, & Pauldrach 1997), so that the evolution of any one of them is of little consequence. However, a variety of selection effects might also bias this interpretation; see, e.g., Oskinova et al. (2001). At a fundamental level, spatially localized variations in the X-ray flux may be difficult to detect against the background contributions collected from nearly the entire volume of the wind.

This situation changed dramatically with the launch of the *Far Ultraviolet Spectroscopic Explorer (FUSE)* satellite, which provides routine access to the resonance lines of O VI. Observations of these wind features permit more sensitive searches for variability, primarily because they are formed by the resonant scattering of photons in localized regions of the wind (i.e., the column of material projected against the disk of the star). Such observations also permit wind features to be identified, even though they are otherwise difficult to detect because of blends with strong stellar and interstellar lines. Moreover, the *FUSE* spectrographs are themselves very sensitive, so that OB-type stars in the Magellanic Clouds are easily accessible.

In order to exploit this new capability, we designed several Principal Investigator (PI) Team programs to obtain sparse time series observations for a large sample of OB-type stars in the Milky Way and Magellanic Clouds. These time series were obtained by breaking long integrations into two or three observations separated by intervals that typically amounted to a few days. Although these time series provide the bare minimum of information required to detect variations, they permitted a broad range of stellar parameters to be surveyed. The aim was to provide a rudimentary assessment of the frequency of O VI variability as a function of spectral type and luminosity class; to determine whether O VI was as variable as the stellar wind features in P V and S IV; and to glean whatever information possible about the nature of the variations. Although this approach is statistical in nature, it complements other studies undertaken with *FUSE* designed to characterize stellar wind variability in O VI and other far ultraviolet wind lines for specific targets (e.g., Fullerton et al. 2003). It also provides the information required to assess the effect of stellar wind variability on measurements of the interstellar O VI lines (see, e.g., Lehner et al. 2001).

2. *FUSE* OBSERVATIONS

2.1. *The sample*

In Tables 1 and 2, we summarize the Milky Way (MW) and Magellanic Clouds (MC) observations, respectively. Basic properties (Galactic coordinates, spectral-type, magnitude and reddening, terminal⁶ and projected rotational velocities) are indicated. Columns 7 and 8 show the separation in days between two successive observations and the dates when they were taken, respectively. Most of these sparse time series consist of 2–3 observations separated by intervals ranging from a few days to several months. The ninth column identifies the rootname of the *FUSE* data set, and is followed by remarks concerning the presence of radial velocity variations in the object.

The time-series observations were obtained mainly

through two large programs conducted by the *FUSE* PI Team, namely the “O VI ISM” (P101, P102, P122) and “hot stars” (P117) working group investigations. The purposes of these multiple observations were to investigate the O VI time-variability in the winds of early-type stars from a stellar point of view (this paper) and to assess its impact on the interstellar absorption measurements of O VI (Lehner et al. 2001). Other (non-proprietary) data from Guest Investigator programs were also included (observation rootnames starting with A and B), as were targets obtained as early-release observations (rootnames starting with X).

Table 1 indicates that the MW sample is strongly biased toward later type stars (O9-B0-B0.5), while the MC sample (Table 2) is slightly more uniformly distributed but of smaller size. These selection effects limit the conclusions that can be drawn: the sample is biased in spectral type; it is not large enough for a meaningful statistical analysis to be performed for each spectral and luminosity class; and the number of multiple observations is very small. It is nonetheless the largest sample available to study O VI variability in the winds of early-type stars. A total of 66 stars (44 Galactic stars, 20 LMC stars, and 2 SMC stars) were observed with typically 2 or 3 observations, except for a few cases with 4 exposures. A future complementary study will involve the analysis of the high time-resolution observations of two LMC stars (Fullerton et al. 2003).

2.2. *FUSE Instrument and Data Reduction*

FUSE consists of four co-aligned telescopes and spectrographs, termed “channels”, two of which have SiC coatings to maximize the sensitivity in the wavelength range $\sim 905\text{--}1105$ Å, while the other two have Al-LiF coatings for sensitivity in the $\sim 1000\text{--}1187$ Å range. This wavelength region provides access to a rich suite of resonance and excited lines, in particular for the ions considered here: O VI, S IV, and P V. The channels are referred to as SiC 1 and SiC 2 and LiF 1 and LiF 2, respectively. This design includes overlap at certain wavelengths, which helps to distinguish between real features in the spectra and instrumental artifacts, particularly fixed-pattern noise. Since we are interested in time-variability in the spectra, this redundant coverage is essential to make sure the differences are in the spectrum of the source and not due to detector defects. More complete descriptions of the design and performance of the *FUSE* spectrographs are given by Moos et al. (2000) and Sahnou et al. (2000), respectively.

Most of the observations were obtained through the $30'' \times 30''$ (LWRS) apertures, except for a few cases where they were obtained through the $4'' \times 20''$ (MDRS) and $1''.25 \times 20''$ (HIRS) apertures. Since flux can be lost through the narrower apertures, systematic multiplicative corrections were applied to adjust the flux levels to a common value. These corrections do not affect the detection of variations. In a few cases, however, and especially for LiF 1B or LiF 2A (which contain the P V lines), the adjustments are compromised by contamination from the “worm,” a feature that deforms the continuum non-linearly. The worm is understood to be due to shadowing from grid wires in front of the detector (Sahnou et al.

⁶ The terminal velocity of a stellar wind is defined as the velocity of outflowing matter at large distances from the star, where it is no longer experiencing significant acceleration but is not yet interacting with the interstellar medium (e.g., Prinja et al. 1990).

2002).

Standard processing with version 2.0.5 of the CALFUSE calibration pipeline software was used to extract and calibrate the spectra. The software screened the data for valid photon events, removed burst events, corrected for geometrical distortions, spectral motions, satellite orbital motions, and detector background, and finally applied flux and wavelength calibrations. The extracted spectra associated with the separate exposures of a given observation were aligned by cross-correlating the positions of strong interstellar lines, co-added, and rebinned to a spectral resolving power of $\sim 15,000$ ($\sim 20 \text{ km s}^{-1}$).

2.3. The Ions Under Study: O VI, S IV, and P V

To compare to wind variability in O VI, we chose to examine the lines of S IV and P V based on two main criteria: (i) They are present over a wide range of spectral types (i.e., S IV and P V are dominant ionization stages or near dominant ionization stages, see below). (ii) The lines fall in sections of the spectrum where they are minimally contaminated by blending with interstellar features. At wavelengths below 1000 \AA , the signal-to-noise level becomes significantly weaker because the effective areas of the SiC channels are smaller.

Below, we briefly recall some properties of the ions under consideration and their behavior through the H-R diagram of OB-type stars. This is mostly based on the two recent *FUSE* atlases of OB-type stars in the MW (Pellerin et al. 2002) and the MC (Walborn et al. 2002).

Owing to the high ionization required to form O VI (I.P.: 113.9–138.1 eV), the O VI $\lambda\lambda 1031.926, 1037.617$ resonance doublet is the most useful tracer of high-energy processes in the optical/UV region of the spectrum. Its prevalence is believed to be directly related to the distribution of X-rays in the winds of the hot stars. In this sense, O VI is often referred to as a “super-ion” (see, e.g., Massa et al. 2003). Other super-ions exist in FUV spectra (e.g., N V and S VI), but O VI remains unique because it is two stages above the dominant ionization stage of O IV. Because of this, Auger ionization of O IV is believed to be the dominant process for producing O VI (Cassinelli & Olson 1979).

Throughout the early O-type dwarf stars and from O2 to B0 supergiants, the O VI lines exhibit typical P Cygni profiles (Pellerin et al. 2002), which consist of an extended blue-shifted absorption trough and red-shifted emission peak. Because the separation between the O VI lines is only 1650 km s^{-1} , the absorption trough of O VI $\lambda 1038$ is often blended with the emission part of O VI $\lambda 1032$. Similarly, the absorption trough of O VI $\lambda 1032$ can be lost in the saturated absorption line of H I Ly β . Moreover, several other interstellar absorption lines (C II, O VI, and H₂) can complicate the appearance of stellar O VI line profiles. We discuss the different contaminations of the wind profiles in more detail in Section 2.4. One should refer to the normalized spectra in the MC *FUSE* atlas of OB-type stars (Walborn et al. 2002), and to the unnormalized spectra of the MW *FUSE* atlas of OB-type stars (Pellerin et al. 2002) for illustrations of these spectra as a function of spectral type.

P V $\lambda\lambda 1117.977, 1128.008$ (I.P.: 51.4–65.0 eV, similar to He II) is a resonance doublet expected to be near the dominant ionization stage in the winds of O-type stars (Massa et al. 2003). It weakens substantially in spectra of B0 and later type stars, for which P IV becomes the dominant ion. Even though it is a dominant ion, it remains unsaturated because of its very low cosmic abundance ($12 + \log[\text{P}/\text{H}] = 5.57$ compared to 8.87 for O and 7.27 for S). This doublet has a luminosity dependence. In mid-O spectra, it appears mainly as photospheric absorption in dwarfs, a weak P Cygni profiles in giants, and strong P Cygni profiles in supergiants (Pellerin et al. 2002).

S IV $\lambda\lambda 1062.664, 1072.973$ (I.P.: 34.8–47.3 eV) is one stage below the expected dominant ion stage of S in the winds of early O-type stars, but starts to dominate in late O and early B-type stars. S IV $\lambda 1063$ is a resonance line, while S IV $\lambda 1073$ arises from low-lying excited levels that produce two transitions at wavelengths 1072.973 and 1073.516 \AA . Since the transition at 1072.973 \AA is about 9 times stronger than the transition at 1073.516 \AA , we consider only the transition at 1072.973 \AA . These transitions have a similar luminosity effect to the P V doublet for mid-O spectral types. However, in the spectra of early B-type stars, the S IV lines are nearly independent of luminosity (Pellerin et al. 2002).

We note that even though the ion fraction of both P V and S IV could be substantially larger than the ion fraction of O VI, their low abundance (0.05% and 2.5% as abundant as O, respectively) could make their detection difficult, especially in the MC where the metallicity is down by about $\gtrsim 50\%$ compared to the MW.

2.4. Detecting Time-Variability with FUSE

Several careful steps were taken to uncover time-dependent changes in the profiles of these sparse time series observations:

(i) For each species, we first transformed the spectra from wavelength space to velocity space in order to facilitate direct comparisons between the components of the doublet and lines from different species. This velocity is in the heliocentric frame, but, unfortunately, the velocity zero point in *FUSE* spectra remains uncertain by several tens of km s^{-1} . The relative velocity can be accurate to a few km s^{-1} within one channel, but can vary by more than 10 km s^{-1} between channels. Using the velocity scale, we compared both the calibrated fluxes and the ratio of the fluxes.

(ii) The blue component of the O VI doublet is affected by the airglow emission and the interstellar absorption of H I Ly β , which lies 1805 km s^{-1} blueward of O VI $\lambda 1032$. In Tables 1 and 2, we give the terminal velocity, v_∞ , which should give roughly the extent of the wind profiles.⁷ When v_∞ is greater than 1805 km s^{-1} , the blue component of the O VI doublet is completely absorbed by the interstellar H I Ly β line. Therefore, the O VI $\lambda 1038$ component was first checked for possible variations. If the ratio of the fluxes in the time series is a horizontal line, we conclude that the wind profiles were the same at the times when the observations occurred. Note that for the red component of the doublet there is generally no information at velocities

⁷ Positions in the absorption trough of a P Cygni profile occur at negative (blueshifted) velocities. To simplify the notation, we have expressed them as positive quantities; i.e., multiplication by -1 is implied.

below 400–500 km s⁻¹ because of blending with the saturated interstellar C II λ 1036 line.

(iii) If there were significant changes in the wind profiles between the different observations, we cross-checked that the profiles (and the ratio of the fluxes) were the same in the redundant spectra extracted from different channels of the observations. The O VI $\lambda\lambda$ 1032, 1038 resonance doublet appears in LiF 1A, LiF 2B, SiC 1A, and SiC 2B spectra. Because the mirrors and gratings move slightly and can be misaligned, information in one channel is occasionally lost, but usually there is more than one channel available. This step is especially important with *FUSE* observations because the aging of detector components can introduce shifts and distortions in the spectral features (known as the “walk”) that could mimic the variations we are looking for. However, this effect is larger near the edge of detector segments SiC 1A and SiC 2B and rather small near the center of detector segments LiF 1A and LiF 2B. The walk problem is also not expected to occur at the same position with the same amplitude in the different detector segments. Thus, by carefully comparing the wind profiles from different segments, we can determine if the observed variation is intrinsic to the stellar wind.

(iv) Further information comes from the O VI λ 1032 transition when this line is not too contaminated by the H I Ly β airglow or absorption or O I airglow. We required that when O VI λ 1032 is available, it exhibits similar variations at the same velocities as the λ 1038 component. If the wind profiles are unsaturated, we can also check that the line strength of O VI λ 1032 is approximately twice the value of O VI λ 1038, as expected for optically thin absorption. Since the velocity separation between the O VI doublet is only 1650 km s⁻¹, there are cases where the wind profiles can overlap.

(v) Similar procedures applied for S IV and P V, but because the doublet separations of these species are much larger than for O VI (2900 and 2480 km s⁻¹, respectively), there is generally no problem of overlapping wind profiles. There is also less blending with saturated interstellar lines. When strong H₂ lines are present, they can contaminate S IV λ 1073 at velocities greater than 2000 km s⁻¹ and S IV λ 1063 at velocities less than 200–500 km s⁻¹. For P V, there are generally no saturated interstellar lines, but possible blends with photospheric O IV $\lambda\lambda$ 1122.3, 1124.9 and Si IV $\lambda\lambda$ 1122.5, 1128.3 can complicate the interpretation of these profiles. We note that the variations of S IV λ 1073 generally appear larger than for S IV λ 1063, contrary to the expectation based on their rather similar oscillator strengths. A similar problem with the relative oscillator strengths of these transitions was noted by Massa et al. (2003).

These procedures ensured that the observed variations occur in the stellar wind profile, and also that weak variations could be detected in spectra characterized by signal-to-noise ratios of ~ 20 . Figure 1 shows 3 examples from the Galactic sample, for which we overplotted the spectra taken at two or three different times. The differences of these fluxes are also plotted for O VI $\lambda\lambda$ 1032, 1038, S IV $\lambda\lambda$ 1062, 1073, and P V $\lambda\lambda$ 1118, 1128 versus velocity. In the following figures, we instead plot $\Delta\tau \equiv \ln[F(t_1)/F(t_2)]$ as a function of v , which has more physical meaning than a flux difference because it is related to the optical depth

of a wind absorption .

The left-hand panel of Figure 1 shows an example where no variation is detected. We note a slight change in the difference of the profiles around -3100 km s⁻¹, probably near the terminal velocity of this star. However, no such change is observed in spectra from other segments, and we therefore rule out wind variability in this case. The right-hand panel shows a large amplitude variation that extends over a large fraction of all profiles. The middle panel shows a very small variation that extends over ~ 500 km s⁻¹ only in the O VI profile. In this case the redundant information provided by both components of the doublet permits small variations in comparatively noisy spectra to be detected unambiguously. Note that in both the middle and right-hand panels, the effect of the worm can be observed in P V λ 1128 for velocities > -1000 km s⁻¹. Yet by following the above procedure, we can distinguish between wind variability and instrumental artifacts. See also Lehner et al. (2001) for other examples.

2.5. Radial Velocity Variations

Wholesale shifts in the positions of photospheric lines indicate systematic motion of the star, possibly in a binary system. Such motion produces a characteristic “S” shape in ratios or differences of spectra at a location that depends on the shift in radial velocity between the two spectra, and over a wavelength region that depends on the width of the photospheric line. We typically noted variations of this sort near the systemic velocity of the star, which indicates only small radial velocity variations. Figure 2 (upper-left panel) shows an example of such an “S”-shape near the systemic velocity (0 km s⁻¹) in the profiles of S IV and P V, which are largely photospheric. These variations are not seen in the O VI line, which instead shows substantial variations between -1550 and -750 km s⁻¹; i.e., in the outflowing wind. An entry of “RV var” (RV var?) in the last column of Tables 1 and 2 indicates the presence (suspected presence) of photospheric radial velocity variations in the *FUSE* time series.

3. TIME DEPENDENCE IN THE O VI WIND PROFILES

In Figure 2, the logarithm of the ratio of the fluxes observed at different times is presented as a function of the velocity for 4 examples in the MW and in the LMC, for O VI $\lambda\lambda$ 1032, 1038, S IV $\lambda\lambda$ 1062, 1073, and P V $\lambda\lambda$ 1118, 1128. Based on analogous figures constructed for the whole sample, we summarize in Table 3 our assessment of whether the wind profiles for these ions were variable at the time of these observations. We also indicate the velocity range over which the variation is observed. In some cases, the high velocity value for O VI was derived using the other species as there is overlap of the O VI wind profiles at velocities larger than 1650 km s⁻¹. For some cases – particularly in the MC sample – no information is given concerning the velocity extent of the O VI wind variations due to uncertainties resulting from the lower signal-to-noise of the data and the greater degree of contamination by H I and O I airglow emission lines. The “(n)” in Table 3 indicates that the spectra suffer either from low signal-to-noise level or some problem in the fluxes, or that the wind is contaminated by other stellar lines (in the case of radial velocity variables, and particularly for the P V

lines). Thus when “(n)” is listed, detections of variability are more uncertain.

Several inferences can be drawn from these measurements:

(1) For the whole sample, 56% of the O VI wind profiles vary with time. For the MW 24/44 (55%) and 13/22 (59%) for the MC show variability. The frequency of O VI wind variability is therefore similar in both samples. If we remove 8 stars with spectral type later than B1 for which O VI is unlikely to be present (Morton 1979; Cassinelli & Olson 1979; Zsargó et al. 2003), 64% of the combined sample is variable. In contrast, only 15% and 5% of the whole sample vary in the wind profiles of S IV and P V. These latter percentages should be treated cautiously because the strengths of these ions vary with spectral type and luminosity class (see § 2.3). They are expected to be strong in the winds of supergiants, and for those stars, the profiles are often variable (see Tables 1 and 2).

(2) Figure 3 shows the fraction of stars for which we observed O VI wind changes as a function of spectral types and luminosity classes, where the error bars are $1/\sqrt{N}$, with N the total number of stars in a given bin. The sample is not large enough to draw any definite conclusions, but suggests that the incidence of O VI variability increases for earlier spectral types. This, however, could also be a selection effect caused by the stronger appearance of the P Cygni profiles in the earlier-type stars.

When all the spectral types are considered, all luminosity classes have a similar percentage of O VI wind variability. However, if we take a more homogeneous sample and consider only spectral types between O9 and B0.5, we find that the O VI wind profiles vary in 7/10 (70%) cases for supergiant stars (luminosity class I), 8/12 (67%) cases for giant stars (luminosity class II-III), and 6/13 (46%) cases for the dwarf stars (luminosity class IV-V). The results are, however, not statistically significant at the 1σ level, and are insufficient to claim that O VI wind variability occurs more frequently in supergiant and giant stars compared to dwarfs. We note that for S IV and P V, variability is observed only in supergiants (except one case observed in a class II star). This is not surprising because in less luminous stars these lines are predominantly photospheric.

(3) From Table 3, the full-width of the variation in the O VI profiles ranges from approximately 225 km s^{-1} to 2200 km s^{-1} , but most fluctuations occur between $\sim 400 \text{ km s}^{-1}$ and 1100 km s^{-1} . The sample is not large enough to study spectral type or luminosity dependence; but in any case no dependence is indicated.

(4) The strength and velocity of the variation can change over times as short as ~ 1 day. However, detailed observations with high-time resolution are required to characterize the time scales rigorously.

(5) In Figure 4, the full-width of the observed variations (Δv), and the maximum absolute radial velocity where significant variability occurs (v_{max}) are plotted as a function of v_{∞} . To investigate possible correlations, we used the Spearman rank-order correlation test, which has the advantage that the statistical significance of a non-zero rank correlation can be quantified reliably without any assumption concerning the distribution of uncertainties. We denote the rank-order correlation coefficient by r , and its statistical significance by t . The statistical significance is

defined in the interval $[0,1]$, where small values indicate greater significance.

Although the top panel of Figure 4 suggests some correlation between Δv and v_{∞} , the Spearman’s correlation test gives $r = 0.73$ with $t = 0.016$ (for the MW sample; $r = 0.46$ with $t = 0.085$ for the whole sample). The width over which the wind profile of the O VI varies is only weakly correlated with the terminal velocity. A least-squares fit to the MW sample gives $\Delta v = (0.42 \pm 0.13) v_{\infty} + (170 \pm 245) \text{ km s}^{-1}$ with a minimum $\chi^2 = 13.7$ and a goodness of fit of 0.09.

In contrast, there is a significant correlation between v_{max} and v_{∞} as $r = 0.92$ with $t = 1.6 \times 10^{-4}$ (for the MW sample; $r = 0.85$ with $t = 6.4 \times 10^{-5}$ for the whole sample). A least-squares fit to the data (MW and MC) gives $v_{\text{max}} = (0.90 \pm 0.11) v_{\infty} + (152 \pm 140) \text{ km s}^{-1}$ with a minimum $\chi^2 = 9.5$ and a goodness of fit of 0.31. The trend is close to the 1:1 relationship as illustrated in Figure 4.

(6) The absolute optical depth variation can be characterized approximately by defining $\Delta T \equiv |\Delta\tau_{\text{high}} + \Delta\tau_{\text{low}}|$, where $\Delta\tau_{\text{high}}$ is the maximum positive logarithmic ratio of the fluxes observed at a specific velocity, and $\Delta\tau_{\text{low}}$ is the maximum absolute negative logarithmic ratio of the fluxes associated with the variation. We find a wide range of values for O VI $\lambda 1032$: $0.4 \lesssim \Delta T \lesssim 1.0$. The detection of $\Delta T \lesssim 0.1\text{--}0.2$ is precluded by the noise level in these data.

(7) $\Delta\tau$ does not seem to depend on the luminosity class or spectral type of the star (see Figure 2). The largest values of $\Delta\tau$ are observed for stars in the LMC. (Note that the y -scale in Figure 2 is larger for the LMC compared to the MW.)

4. O VI WIND ABSORPTION FEATURES

In the previous section, we assessed the frequency of variability in the O VI wind line for many OB-type stars. Extensive studies of the winds through ultraviolet resonance lines in other species show that narrow or discrete absorption components (DACs) are associated with the extended absorption troughs (for a recent review, see Prinza 1998). These DACs become particularly strong near v_{∞} . The typical P Cygni profiles observed for lower ionization stages (e.g., C IV, Si IV) are also observed for the O VI doublet (Pellerin et al. 2002; Walborn et al. 2002). Figure 5 shows that strong, high velocity absorption components are also observed in O VI.

Several pieces of evidence confirm that these absorptions occur in the wind: (i) no strong photospheric lines were identified in this region of the spectrum (we note, however, potential photospheric Fe III and P III lines that can contaminate the O VI spectrum for the later type stars; see Zsargó et al. 2003); (ii) the velocity of the features changes from one observation to the next (for the best case see Figure 3 in Lehner et al. 2001); (iii) both components of the O VI doublet can be observed (see Figure 5 and Lehner et al. 2001); and (iv) in cases of a binary, aligning the photospheric lines do not align these features. The projected rotational velocity also broadens the photospheric lines, and there is no correlation between the width of these absorption features and the $v \sin i$ values listed in Table 1. Finally, these high-velocity features do not have an interstellar origin because in some cases they are too

broad. Furthermore, transient features are not commonly observed in the interstellar gas. These features are therefore due to O VI absorption in the stellar wind.

In Table 4, we present the stars for which we observed unambiguously the O VI wind absorption features and their blue-shifted velocities, v_{abs} , which correspond to the deepest part of these features.⁸ (When the feature has a flat bottom, its centroid is used). The last column also presents the strength of these features, classified as weak, medium and strong. A “weak” (small width and small optical depth) absorption corresponds to features as observed in the spectra of HD 161807; a “medium” (intermediate) absorption corresponds to features as observed in the spectra of CPD-72°1184; and a “strong” (large width and large optical depth) absorption corresponds to features as observed in the spectra of HD 92554 (see Figure 5). Sometimes weak and strong features are observed in the same spectrum. This is the case, e.g., for HD 168941, for which the O VI $\lambda 1038$ wind feature is blended with the O VI $\lambda 1032$ absorption interstellar line. We take this qualitative approach rather than a quantitative approach because the continuum is very uncertain for these generally complex features (but see Zsargó et al. 2003 for a more quantitative approach).

Below we summarize the properties of these O VI wind absorption features:

(1) They are observed in 33% of our sample (34% in the MW, 32% in the MC), in the spectra of stars with spectral types from O7.5 to B0.5 and in every luminosity class. Since strong absorption components are preferentially found near v_{∞} (see point 4 below) they are especially difficult to detect for stars with $2400 \lesssim v_{\infty} \lesssim 3400$ km s⁻¹ owing to blending with the strongly saturated interstellar H I Ly β line. Stars with such terminal velocities range from O3 to about O7-O8 (Prinja et al. 1990). Furthermore, these stars typically exhibit strongly saturated P Cygni profiles in the O VI resonance lines, which makes the detection of localized absorption enhancements all the more difficult. A similar problem arises when $v_{\infty} \lesssim 600$ km s⁻¹ because of the contamination of the wing of interstellar H I Ly β and C II absorption lines. Stars with such terminal velocities typically have spectral types later than B0.5 (Prinja et al. 1990).

(2) Their shapes are usually not Gaussian and can be asymmetric.

(3) They appear with different strengths, and their full-widths at half maximum vary approximately from less than 100 km s⁻¹ up to 400–500 km s⁻¹, the latter generally being observed near v_{∞} (see point 4).

(4) For the strong features, v_{abs} is similar to v_{∞} ($0.9 v_{\infty} \lesssim v_{\text{abs}} \lesssim v_{\infty}$, except for Sk -67°05 where $v_{\text{abs}} \approx 0.7 v_{\infty}$), while for weak and medium features, v_{abs} is generally red-shifted by a few hundred km s⁻¹ with respect to v_{∞} ($0.7 v_{\infty} \lesssim v_{\text{abs}} \lesssim 0.9 v_{\infty}$; except for Sk -67°101 where $v_{\text{abs}} \approx 0.5 v_{\infty}$).

(5) Some features appear to vary on time scales of a day, but other features are at the same velocity after several days or months have passed.

(6) The sparse time-series observations suggest that these features accelerate slowly with an acceleration of $\sim 10^{-3}$ to less than $\sim 10^{-4}$ km s⁻² (see Figure 5 and Figure 3 in Lehner et al. 2001).

(7) There is no direct relation between the widths of these features and the $v \sin i$ of star. Neither their width nor strength correlates with luminosity class or spectral type.

(8) There is no systematic difference in the frequency of occurrence between the MW and MC sample, though the size of the sample is certainly not large enough to draw any definitive conclusions.

5. DISCUSSION AND SUMMARY

We have described a survey for stellar wind variability based on sparse time-series observations of a large sample of stars observed with *FUSE*. This survey demonstrates that the winds in OB-type stars are variable in the O VI doublet on various scales both in time and velocity. The typical signatures of wind variability are observed via (i) variation in the profiles for 56% of the spectral types from O3 to B3 and 64% of the spectral types from O3 to B1, and (ii) wind absorption features in 33% of the cases for the whole sample, or 46% of the cases for spectral types from O3 to B0.5.

These percentages have to be considered lower limits. Owing to the nature of this survey, only a few exposures separated by a few days or a few months were obtained with no regard to the time scales believed to be relevant to the variability of hot-star winds. Furthermore, the quality of *FUSE* data precludes the detection of small-amplitude variations. In view of the high incidence of variability detected under these circumstances, variability in O VI wind profiles is likely ubiquitous.

At spectral types later than B1, no O VI wind variability is observed. This could be due to limitations in the detectability of wind activity caused by the weakness or absence of this feature in these stars, as well as the smaller number of stars observed in those spectral types. In the former case, this might be explained by the fact that for later spectral types, O III becomes the dominant ion, so that O VI cannot be produced via Auger ionization (Cassinelli & Olson 1979).

The sample is not large enough to relate the frequency of the temporal variations or the absorption features to specific spectral types or luminosity classes. But it suggests that stars with spectral types earlier than O8 may show variations more often.

The observed variations extend over several hundreds of km s⁻¹ and can be strong. This favors the idea that the bulk of the X-rays producing O VI via Auger ionization originates from a few strong shocks.

The width over which the wind profile of the O VI varies is poorly correlated with the terminal velocity for the MW sample. There is, however, a significant correlation (close to a 1:1 relationship) between the blue-edge velocity of the variation (i.e., at the maximum (negative) velocity at which no variation is observed) and v_{∞} (see Figure 4). This might imply that systematically stronger shocks oc-

⁸ Not all the stars with absorption features exhibited variability. For these cases, we used the morphological approach described by Zsargó et al. (2003) to determine whether the absorption features were formed in the wind. For a positive detection, we required that DACs be present at the same velocity as the O VI components in archival *IUE* or *HST* spectra of the wind profiles of one or more of the resonance lines of C IV, Si IV, and N V.

cur at larger velocities (i.e., near v_∞).

Although the high velocity absorption features seen in O VI directly indicate the outflow of hot gas, it is not clear from this survey exactly how these absorption features evolve with time. Figure 3 in Lehner et al. (2001) and Figure 5 give nice examples of velocity-varying O VI absorption wind features, but more intensive time-series observations are required to characterize this evolution (see Fullerton et al. 2003). We note, however, that the stronger (both in optical depth and width) components are near the terminal velocity, while weaker components appear and evolve at lower velocities.

By comparing the frequency of variability exhibited by O VI to that seen in S IV and P V, we found that only a small percentage of the whole sample shows wind variations for the lower ions, and those variations are mainly observed in supergiant stars. This may be largely due to two selection effects. One is that S and P are much less abundant than O, thereby making it more difficult to detect variations in these ions. The other is that our sample is biased toward late O-type and early B-type stars, where the wind becomes weaker for P V; i.e., the P V line becomes principally a photospheric line.

The low frequency of observed variability in S IV is harder to understand, because S IV is expected to be the dominant ion in the winds of late O- and early B-type stars. If it is not merely an abundance selection effect, then this result may imply that the highly ionized com-

ponent of these cooler winds is enhanced compared with hotter winds. Suppose, e.g., that the variability exhibited by a wind line is proportional to its optical depth; i.e., $\Delta\tau \propto \tau$. The ionization fraction is $q \propto \tau / (f\lambda A_E)$ (see, e.g., Massa et al. 2002), where A_E is the abundance of the element. Since O VI variability is detected more frequently than S IV variability, $\Delta\tau(\text{O VI}) > \Delta\tau(\text{S IV})$, i.e. $\tau(\text{O VI}) > \tau(\text{S IV})$, and $q(\text{O VI}) > 0.01 q(\text{S IV})$. If S IV is dominant, $q(\text{S IV}) \sim 1$, and hence $q(\text{O VI}) \gtrsim 0.01$, which is at least an order of magnitude larger than typically observed for early- and mid-O type stars (Massa et al. 2003). This evidence for an excessive abundance of O VI in the winds of comparatively cool stars – where it is least expected – is consistent with the predictions of MacFarlane et al. (1994), who concluded that the presence of X-rays can substantially alter the ionization balance of lower-density winds.

This work is based on data obtained for the Guaranteed Time Team by the NASA-CNES-CSA FUSE mission operated by the Johns Hopkins University. Financial support to U. S. participants has been provided by NASA contract NAS5-32985. This research has made use of the NASA Astrophysics Data System Abstract Service and the SIMBAD database, operated at CDS, Strasbourg, France. We thank the referee, Doug Gies, for helpful comments that improved the presentation of these results.

REFERENCES

- Bianchi, L., et al. 2000, *ApJ*, 538, 57
 Cassinelli, J. P., & Olson, G. D. 1979, *ApJ*, 239, 304
 Crampton, D., Bernard, D., Harris, B. L., & Thackeray, A. D. 1976, *MNRAS*, 176, 683
 Cranmer, S. R. & Owocki, S. P. 1996, *ApJ*, 462, 469
 Conti, P. S., Garmany, C. D., & Massey, P. 1986, *AJ*, 92, 48
 Feldmeier, A., Puls, J., & Pauldrach, A. W. A. 1997, *A&A*, 322, 878
 Fitzpatrick, E. L. 1988, *ApJ*, 335, 703
 Fitzpatrick, E. L. 1991, *PASP*, 103, 1123
 Fullerton, A. W., Massa, D. L., Prinja, R. K., Howarth, I. D., Willis, A. J., & Owocki, S. P., in prep
 Garrison, R. F., Hiltner, W. A., & Schild, R. E. 1977, *ApJS*, 35, 111
 Guetter, H. H. 1968, *PASP*, 80, 197
 Harnden, F. R. et al. 1979, *ApJ*, 234, L51
 Hill, P. W. 1970, *MNRAS*, 150, 23
 Hill, P. W., Kilkenny, D., & van Breda, I. G. 1974, *MNRAS*, 168, 451
 Hiltner, W. A. 1956 *ApJS*, 2, 389
 Houck, N., & Cowley, A. P. 1975, Michigan Spectral Survey, Ann Arbor, Dep. Astron., Univ. Michigan, 1
 Houck, N., & Smith-Moore, M. 1988, Michigan Spectral Survey, Ann Arbor, Dep. Astron., Univ. Michigan, 4
 Howarth, I. D., Siebert, K. J., Hussain, G. A. J., & Prinja, R. K. 1997, *MNRAS*, 284, 265
 Jaxon, E. G., Guerrero, M. A., Howk, J. C., Walborn, N. R., Chu, Y.-H., & Wakker, B. P. 2001, *PASP*, 113, 1130
 Karlsson, B., 1969, *Arkiv for Astron.*, 5, 241
 Lehner, N., Fullerton, A. W., Sembach, K. R., Massa, D. L., & Jenkins, E. B. 2001, *ApJ*, 556, L103
 Lennon, D. J. 1997, *A&A*, 317, 871
 MacFarlane, J. J., Cohen, D. H., & Wang, P., 1994, *ApJ*, 437, 351
 MacFarlane, J. J., Waldron, W. L., Corcoran, M. F., Wolff, M. J., Wang, P., & Cassinelli, J. P. 1993, *ApJ*, 419, 813
 Maiz-Apellániz, J. & Walborn, N. R. 2002, in Proc. IAU Symp. 212, “A Massive Star Odyssey, from Main Sequence to Supernova”, ed. K. A. van der Hucht, A. Herrero, & C. Esteban (San Francisco: ASP), 560
 Massa, D. L., Fullerton, A. W., Sonneborn, G., Hutchings, J. B. 2003, *ApJ*, 586, in press
 Moos, H. W., et al. 2000, *ApJ*, 538, L1
 Morgan, W. W., Code, A. D., & Whitford, A. E. 1955, *ApJS*, 2, 41
 Morton, D. C. 1979, *MNRAS*, 189, 57
 Mullan, D. J. 1984, *ApJ*, 283, 303
 Oskinova, L. M., Ignace, R., Brown, J. C., & Cassinelli, J. P. 2001, *A&A*, 373, 1009
 Owocki, S. P., Castor, J. I., & Rybicki, G. B. 1988, *ApJ*, 335, 914
 Patriarchi, P., & Perinotto, M. 1992, *A&A*, 258, 285
 Pellerin, A. et al. 2002, *ApJS*, 143, 159
 Penny, L. 1996, *ApJ*, 463, 737
 Prinja, R. K. 1998, in *Cyclical Variability in Stellar Winds*, ed. L. Kaper & A. W. Fullerton (Berlin: Springer), 92
 Prinja, R. K., Barlow, M. J., & Howarth, I. D. 1990, *ApJ*, 361, 607
 Prinja, R. K., & Crowther, P. A. 1998 *MNRAS*, 300, 828
 Sahnou, D. J., 2002, in *The FUSE Instrument and Data Handbook*, Version 2.0
 Sahnou, D. J., et al. 2000, *ApJ*, 538, L7
 Schild, R. E. 1970, *ApJS*, 161, 855
 Seward, F. D., Forman, W. R., Giacconi, R., Griffiths, R. E., Harnden, F. R., Jones, C., & Pye, J. P. 1979, *ApJ*, 234, L55
 Snow, T. P. & Morton, D. C. 1976, *ApJS*, 32, 429
 ud-Doula, A. & Owocki, S. P. 2002, *ApJ*, 576, 413
 Uesugi, A., & Fukuda, I. 1982, Revised Catalogue of Stellar Rotational Velocities, Department of Physics & Astronomy, Kyoto University
 Walborn, N. R. 1971, *ApJS*, 23, 257
 Walborn, N. R. 1972, *AJ*, 77, 312
 Walborn, N. R. 1973, *AJ*, 78, 1067
 Walborn, N. R. 1976, *ApJ*, 205, 419
 Walborn, N. R. 1977, *ApJ*, 215, 53
 Walborn, N. R. 1982, *AJ*, 87, 1300
 Walborn, N. R., Fullerton, A. W., Crowther, P. A., Bianchi, L., Hutchings, J. B., Pellerin, A., Sonneborn, G., & Willis, A. J. 2002, *ApJS*, 141, 443
 Walborn, N. R., Lennon, D. J., Haser, S. M., Kudritzki, R.-P., & Voels, S. A. 1995, *PASP*, 107, 104
 Zsargó, J., Fullerton, A. W., Lehner, N., & Massa, D. 2003, *A&A*, submitted

FIGURE CAPTIONS:

Figure 1: Examples of *FUSE* spectra for three Galactic stars for the O VI $\lambda\lambda 1032, 1038$, S IV $\lambda\lambda 1062, 1073$, and P V $\lambda\lambda 1118, 1128$ doublets. The spectra and difference spectra are shown in units of $10^{-12} \text{ erg cm}^{-2} \text{ s}^{-1} \text{ \AA}^{-1}$. For HD 64568 (left panel), the observations were separated by 2.5 days; for HD 47417 (middle panel), the observations were separated by 0.8 day, and for HD 210509 (right panel), the observations were separated by 1.4 and 1.3 days. The black, red, and blue profiles denote the first, second, and third observations, respectively. The dotted line in the right panel indicates the terminal velocity of HD 210509. The position of the Lyman β airglow line is indicated in the uppermost panels. The range of variability in the O VI line of HD 47417 is emphasized by vertical red lines in difference flux panel.

Figure 2: The logarithm of the ratio of the fluxes (taken at different times indicated by the Δt in days) vs. velocity for the O VI $\lambda\lambda 1032, 1038$, S IV $\lambda\lambda 1062, 1073$, and P V $\lambda\lambda 1118, 1128$ for 4 stars in the Galaxy and the LMC, showing the variety of variations in the profiles. Note that the y -scale of a panel is the same for a given species but can change from species to species. Vertical dotted lines indicate v_∞ , while the extent of the variation is shown by the solid thick vertical lines. The variation in the profile ratio of S IV and P V in the spectra of HD 187459 at $\sim 0 \text{ km s}^{-1}$ indicates radial velocity variations, perhaps due to motion in a binary system.

Figure 3: Fraction of stars in the combined Galactic and Magellanic Clouds sample exhibiting O VI wind variability for different temperature (left panel) or luminosity classes (right panel). The dotted line represents the average fraction of observed O VI wind variability.

Figure 4: The full-width (Δv , top panel) and blue edge (v_{max} , bottom panel) of the variability observed in the O VI wind with respect to the terminal velocity (v_∞). Triangles correspond to the MW stars, and squares denote stars in the LMC. Typical measurement errors are about 10% for v_∞ and 100–200 km s^{-1} for Δv and v_{max} . The dotted lines indicate a 1:1 relationship. The dashed lines are a least-squares fit weighted by the inverse of the quadratic sum of the errors to the data (only MW sample in top panel, both samples in bottom panel).

Figure 5: O VI absorption components in the wind profiles of early-type stars in the Galaxy. The profiles are plotted in flux units versus velocity with respect to O VI $\lambda 1032$ (panel a) or $\lambda 1038$ (panel b). Δt indicates the time in days between successive observations. Black, red, and blue profiles indicate the first, second, and third observations, respectively. The vertical dotted lines indicate the “centroid” of the O VI DAC. See Lehner et al. (2001) for other examples in the MW and the LMC.

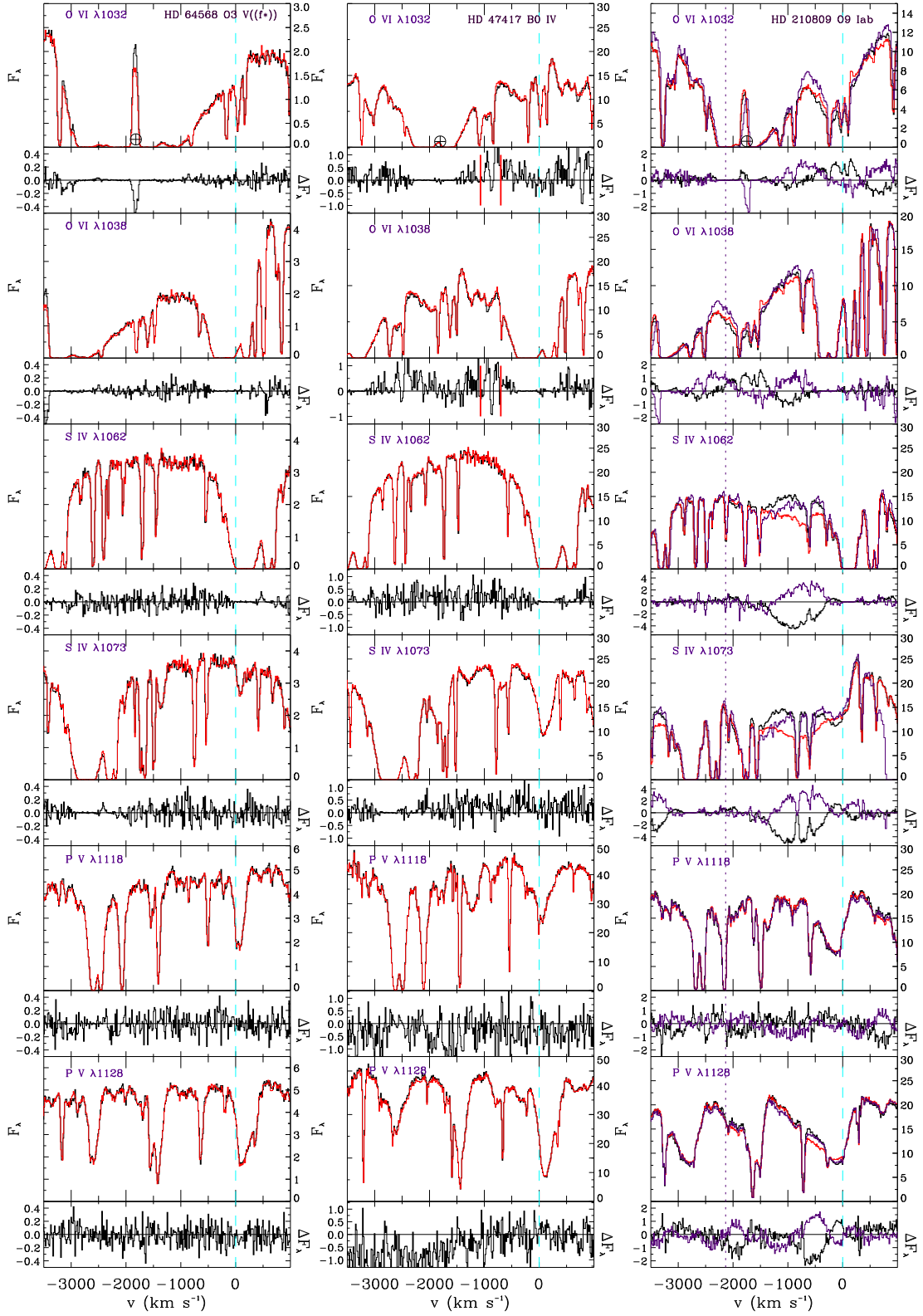


FIG. 1.—

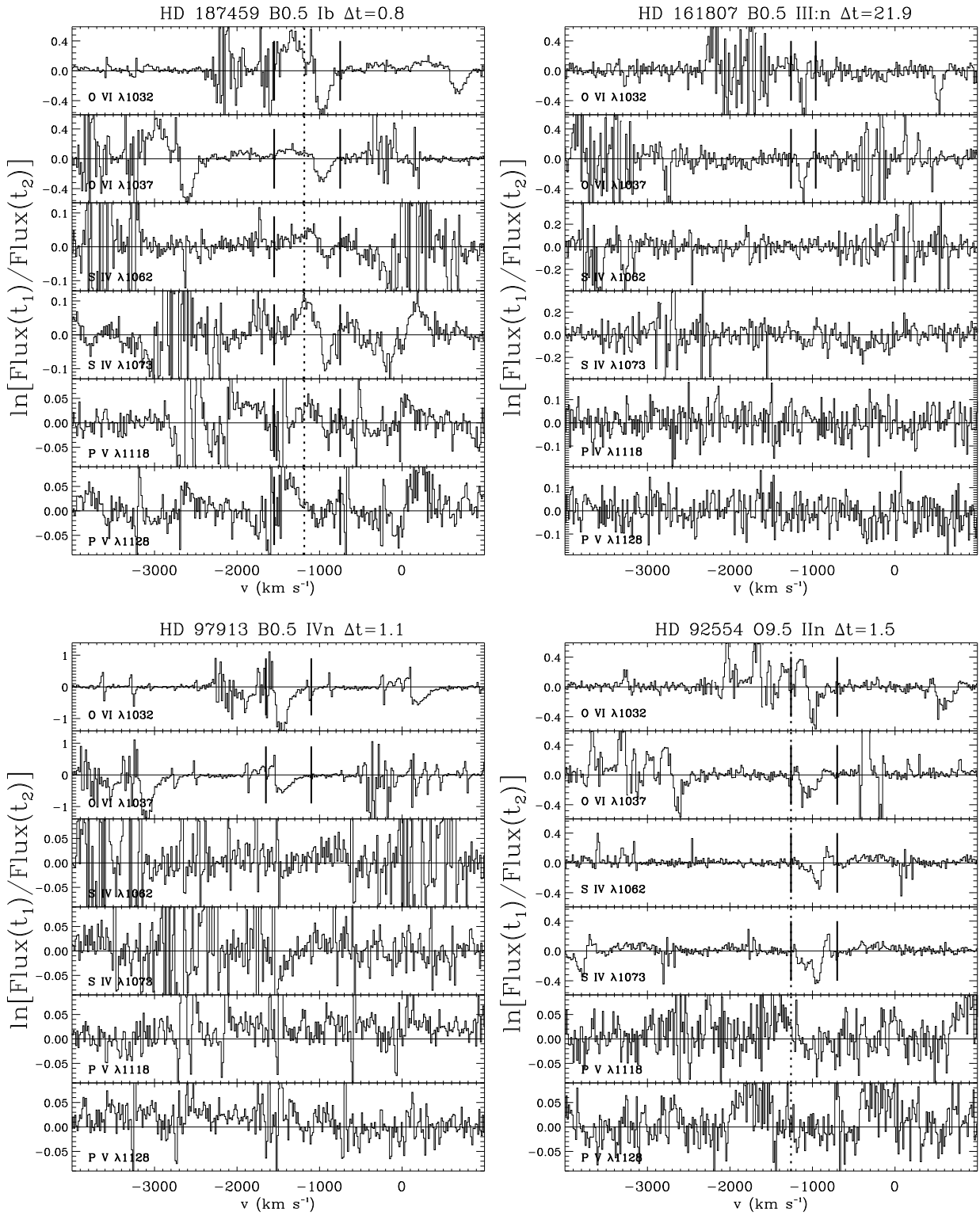


FIG. 2.—

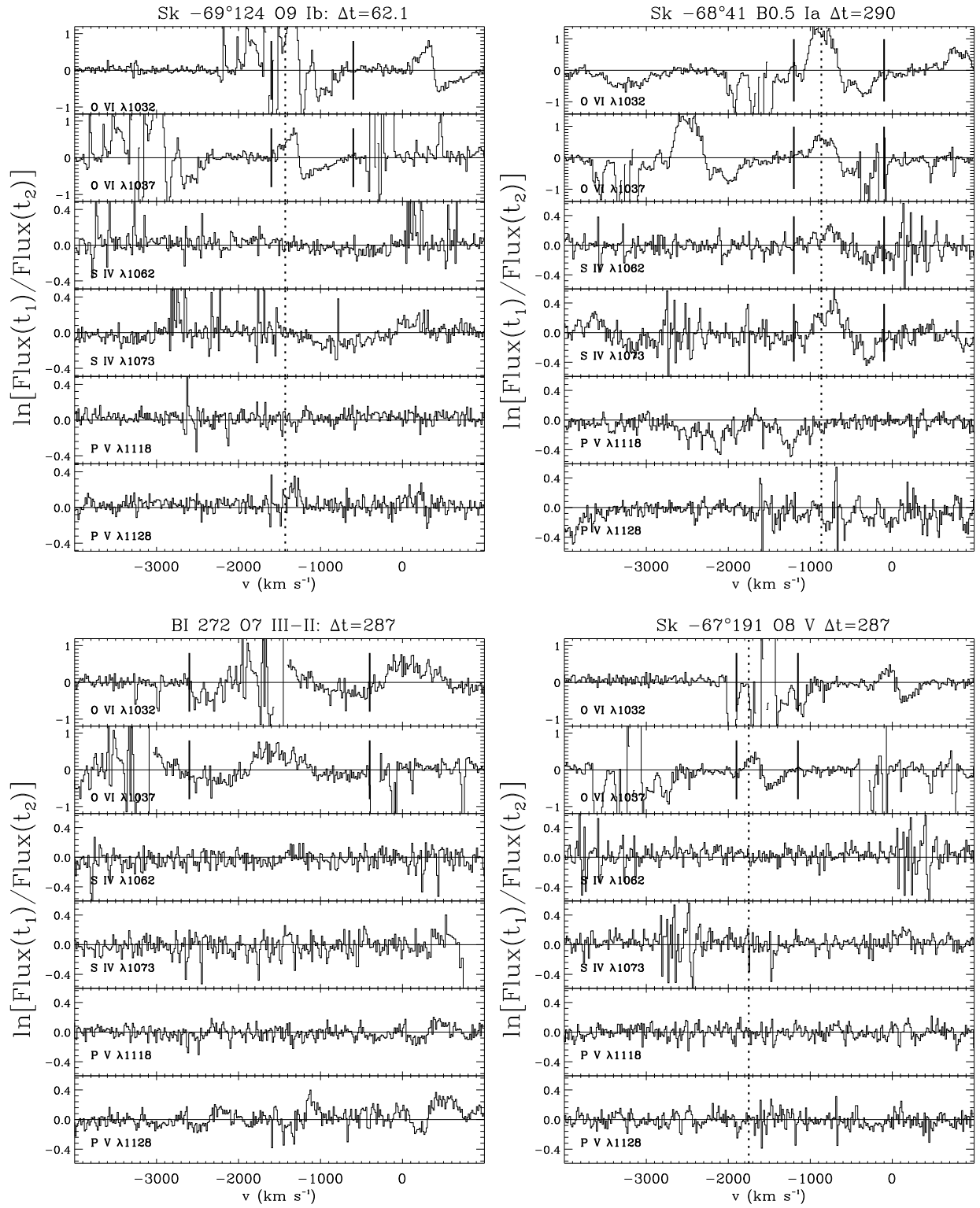


FIG. 2.— Continued. LMC stars.

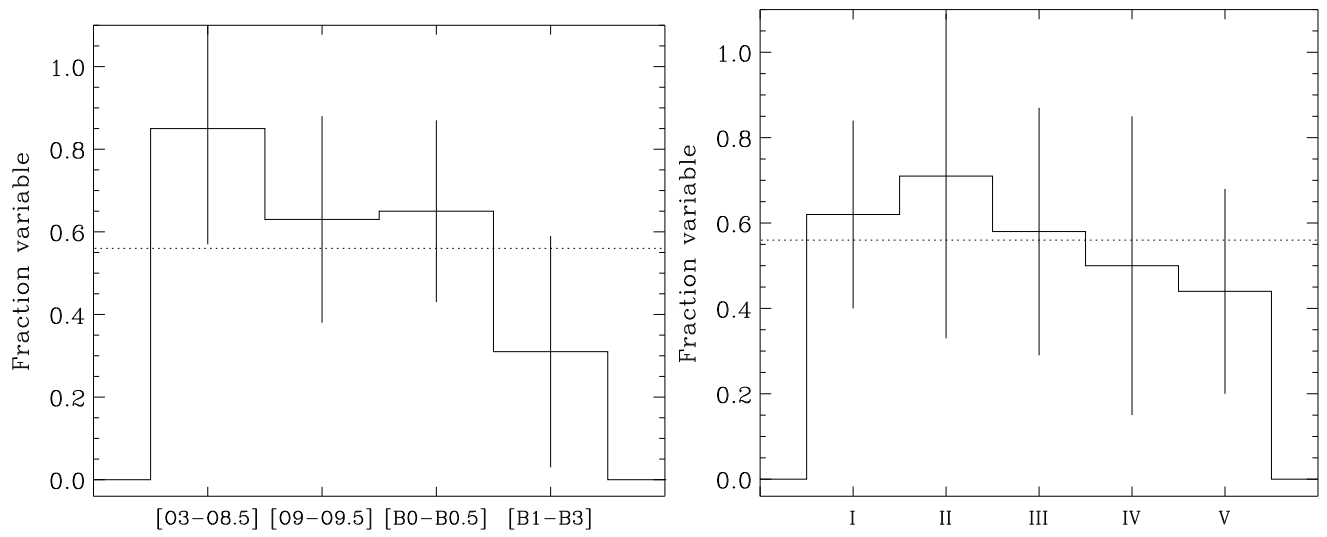


FIG. 3.—

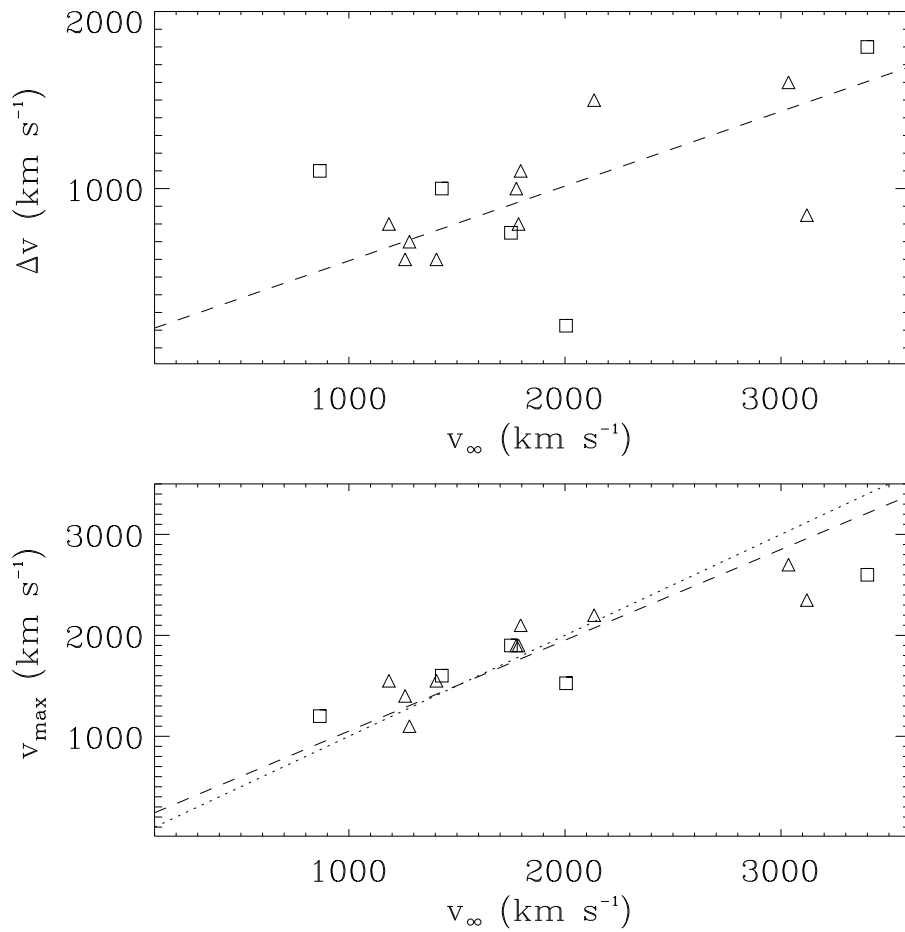


FIG. 4.—

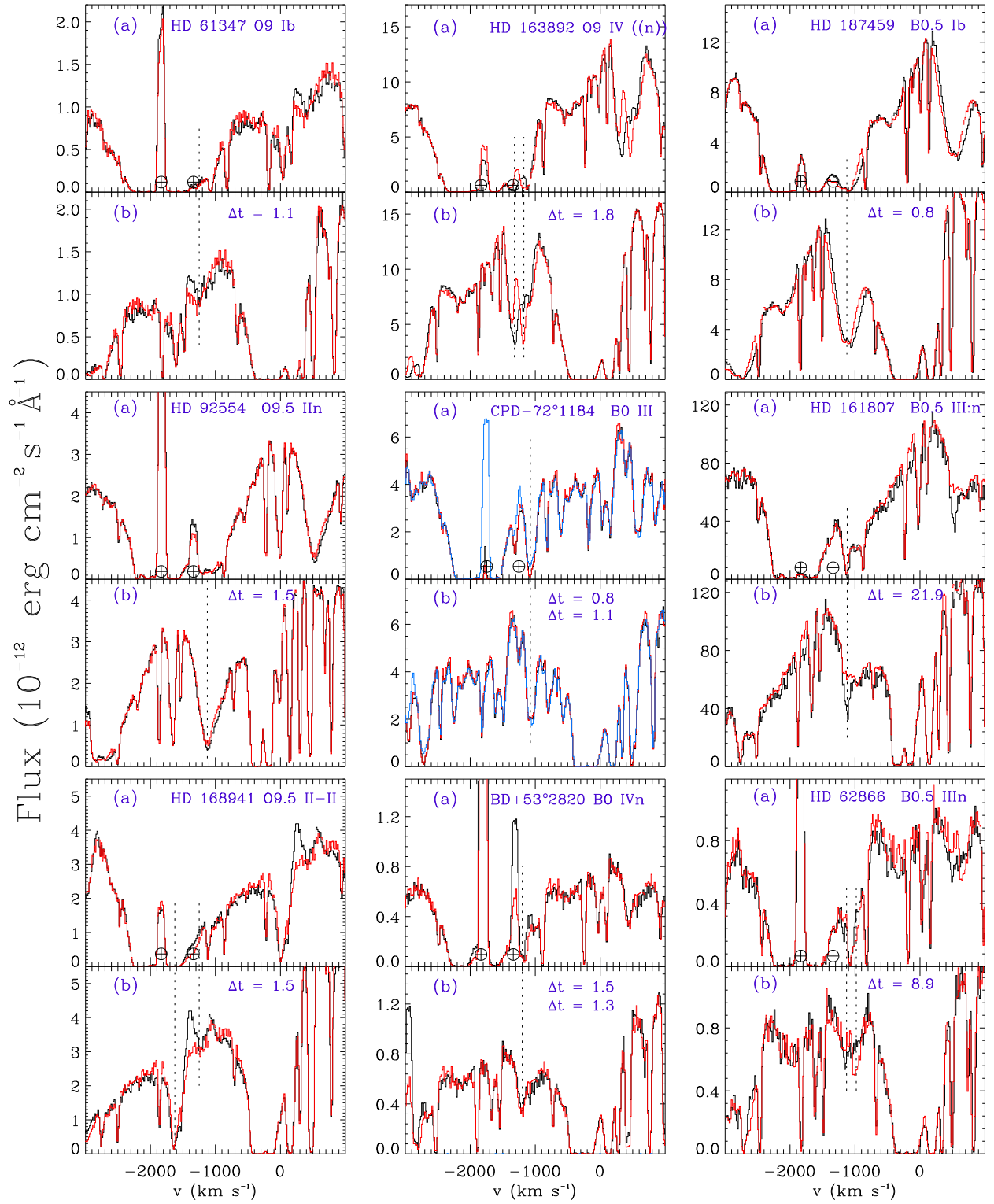


FIG. 5.—

TABLE I
OBSERVATIONS OF GALACTIC STARS

Star	Sp. Type Reference	l ($^{\circ}$)	b ($^{\circ}$)	V $E(B - V)$ (mag.)	$v \sin i$ v_{∞} (km s^{-1})	Δt^a (day)	UT-Date	Rootname	Remarks ^b
HDE 303308	O3 V((f)) W73	287.60	-0.61	8.17 0.45	111 ^b 3035 ^b	1.7	2000-05-25 2000-05-27	P1221601 P1221602	
HD 64568	O3 V((f*)) W82	243.14	+0.71	9.38 0.37	...	2.5 5.7	2000-03-25 2000-04-03 2000-04-05	P1221104 P1221102 P1221103	
CPD-59°2600	O6 V((f)) W73	287.60	-0.74	8.61 0.53	142 ^b 3120 ^b	1.9 1.9	2000-03-21 2000-03-23 2000-03-25	P1221401 P1221402 P1221403	
CPD-59°2603	O7 V W73	202.18	-58.98	8.77 0.46	164 ^{b,\alpha} 1840 ^{b,\alpha}	67.3 17.0	2000-01-30 2000-03-21 2000-04-06	S3040501 P1221501 S3040502	
HD 152590	O7.5 V W72	344.84	+1.83	8.48 0.38	60 ^b 1785 ^b	35.1	2001-07-08 2001-07-12	B0710601 B0710602	RV var
HD 61347	O9 Ib M55	230.60	+3.79	8.43 0.45	116 ^b 1775 ^b	1.1	2000-04-15 2000-04-16	P1022001 P1022002	
HD 210809	O9 Iab W76	99.85	-3.13	7.54 0.33	117 ^b 2135 ^b	1.4 1.3	2000-08-05 2000-08-07 2000-08-08	P1223101 P1223102 P1223103	RV var
HD 153426	O9 II W73	258.07	-15.37	7.47 0.45	108 ^b 2200 ^b	105	2000-03-31 2000-07-14	P1027201 P1027202	RV var
HD 91651	O9 V:n W73	286.55	-1.72	8.84 0.29	292 ^b 1705 ^b	1.3	2000-05-25 2000-05-27	P1023101 P1023102	
HD 92554	O9.5 II:n G77	287.60	-2.02	9.47 0.39	298 ^b 1260 ^b	1.5	2000-05-26 2000-05-27	P1023201 P1023202	RV var?
HD 168941	O9.5 II-III W82	275.23	-3.62	9.34 0.37	116 ^b 1795 ^b	2.2	2000-08-30 2000-09-01	P1016501 P1016502	RV var
HD 156292	O9.5 III W73	345.35	-3.08	7.49 0.56	102 ^b 1355 ^b	1.9	2000-04-03 2000-04-05	P1027402 P1027403	RV var
HD 163892	O9 IV ((n)) W73	7.15	+0.62	7.44 0.47	201 ^b 1405 ^b	1.8	2001-04-27 2001-04-29	P1027601 P1027602	RV var
HDE 308813	O9.5 V S70	294.80	-1.61	9.38 0.37	...	2.0 1.3	2000-03-23 2000-03-25 2000-03-27	P1221901 P1221902 P1221903	RV var
CPD-72°1184	B0 III H74	233.12	-61.63	10.68 0.23	...	0.8 1.1	2000-03-27 2000-03-28 2000-03-29	S5140101 S5140102 S5140103	
HD 192035	B0 III-IV(n) W71	68.81	+3.85	6.44 0.42	155 ^c ...	2.5 2.0	2000-06-17 2000-06-19 2000-06-21	P1028601 P1028602 P1028603	
HD 47417	B0 IV M55	205.35	+0.35	6.97 0.31	...	0.8	2000-03-15 2000-03-16	P1021602 P1021601	
HD 203374A	B0 IVpe M55	100.26	+8.58	6.69 0.60	350 ^c ...	0.4	2001-08-02 2001-08-02	B0300101 B0300102	
BD +53°2820	B0 IVn H56	9.26	+58.16	9.95 0.40	...	1.5 1.3	2000-08-06 2000-08-07 2000-08-08	P1223201 P1223202 P1223203	
HD 191495	B0 IV-V W71	72.74	+1.41	8.26 0.40	235 ^c ...	1.0	2000-08-10 2000-08-11	P1222901 P1222902	RV var
HD 195965	B0 V M55	83.33	+7.76	8.20 0.36	...	141.2 0.9	2000-06-17 2000-11-08 2000-11-09	P1028801 P1028802 P1028803	
HD 186994	B0.2IV W71	78.62	+10.06	7.51 0.20	125 ^c ...	63.4	2001-07-02 2001-09-07	P2160801 P2160802	RV var
HD 207538	B0.2 V MA02	12.12	+64.38	7.31 0.63	51 ^b ...	226	1999-12-08 2000-07-21	P1162902 P1162903	
HD 187459	B0.5 Ib M55	68.81	+3.85	6.44 0.42	139 ^b 1185 ^b	0.8	2000-08-10 2000-08-11	P1028201 P1028202	RV var?
HD 224151	B0.5 II M55	115.44	-4.64	6.00 0.48	115 ^b 1280 ^b	2.1 0.6	2000-08-11 2000-08-13 2000-08-14	P1224101 P1224102 P1224103	RV var
HDE 332407	B0.5 III: W71	64.28	+3.11	8.50 0.48	140 ^c ...	1.8	2000-06-10 2000-06-12	P1222801 P1222802	
HD 161807	B0.5 III:n G77	351.78	-5.85	6.99 0.23	350 ^c ...	21.9	2000-08-17 2000-09-08	P1222301 P1222302	
HD 172140	B0.5 III H70	5.28	-10.61	9.93 0.25	...	1.5 2.1	2000-05-18 2000-05-20 2000-05-22	P1016601 P1016602 P1016603	
HD 62866	B0.5 III:n G77	237.48	+1.80	9.01 0.35	...	8.9	2000-04-02 2000-04-11	P1221002 P1221004	
HD 97913	B0.5 IVn G77	290.84	+1.41	8.80 0.32	310 ^c ...	1.1	2000-05-26 2000-05-27	P1221701 P1221702	
BD +35°4258	B0.5 Vn M55	77.19	-4.74	9.41 0.29	...	3.0	2000-06-14 2000-06-17	P1017901 P1017902	RV var
HD 148422	B1 Ia HC75	329.92	-5.60	8.60 0.28	81 ^b 1335 ^b	2.1 1.9	2000-04-08 2000-04-10 2000-04-12	P1015001 P1015002 P1015003	
HD 191877	B1 Ib M55	61.57	-6.48	6.28 0.18	152 ^b 1160 ^b	420	2000-06-05 2001-07-30	P1028701 P2051101	RV var?
HDE 235783	B1 Ib	101.69	-1.87	8.68	93 ^b	1.5	2000-08-05	P1223301	

TABLE 1—*Continued*

Star	Sp. Type Reference	l ($^{\circ}$)	b ($^{\circ}$)	V $E(B - V)$ (mag.)	$v \sin i$ v_{∞} (km s^{-1})	Δt^a (day)	UT-Date	Rootname	Remarks ^b
	M55			0.36	1070 ^b	1.3	2000-08-07	P1223302	
							2000-08-08	P1223303	
BD +48 $^{\circ}$ 3437	B1 Iab M55	354.70	+58.01	8.69 0.35	54 ^b ...	1.3 1.4	2000-08-06	P1018401	
							2000-08-07	P1018402	
							2000-08-09	P1018403	
HD 225757	B1 IIIIn C76	309.48	+54.50	10.59 0.22	2.0 0.6	2000-08-06	P1017701	
							2000-08-08	P1017702	
							2000-08-09	P1017703	
HD 91597	B1 IIIIne G77	286.86	-2.37	9.84 0.30	1.4 2.3	2000-02-04	P1023002	
							2000-02-06	P1023003	
							2000-02-08	P1023004	
BD +52 $^{\circ}$ 3210	B1 V M55	10.9608	+56.31	10.69 0.24	1.3 1.3	2000-08-06	P1223501	
							2000-08-07	P1223502	
							2000-08-08	P1223503	
HD 73	B1.5 IV W71	114.17	-18.69	8.48 0.07	105 ^c ...	49.9	2000-08-01	P1010101	
							2000-09-20	P1010102	
HD 202347	B1.5 V W71	44.85	+57.17	7.50 0.17	125 ^c ...	84.7	2000-06-20	P1028901	
							2000-09-13	P1028902	
BD +53 $^{\circ}$ 2885	B2 III M55	102.75	-2.93	10.46 0.28	2.7	2000-08-02	P1223601	
							2000-08-05	P1223602	
HD 47961	B2 V K69	203.02	+2.28	7.50 0.08	11.7	2001-02-20	P1310401	
							2001-03-04	P1310402	
HD 51013	B3 V HS88	235.11	-10.13	8.81 0.05	438	2000-01-24	A0630901	
							2001-04-05	A0630902	
HD 47777	B3 V G68	203.12	+2.03	7.90 0.07	135 ^c ...	11.7	2001-02-20	P1310201	
							2001-03-04	P1310202	

^a Δt , time between successive observations.

^bRadial velocity variation detected or suspected.

References. — (a) Sources of spectral type: C76=Crampton et al. (1976); G77=Garrison et al. (1977); G68=Guetter (1968); H56=Hiltner (1956); H70=Hill (1970); H74=Hill et al. (1974); HC75=Houck & Cowley (1970); HS88=Houck & Smith-Moore (1988); K69=Karlsson (1969); M55=Morgan et al. (1955); MA02=Maíz-Apellániz & Walborn (2002); S70=Schild (1970); W71, W72, W73, W76, W82=Walborn (1971, 1972, 1973, 1976, 1982). (b) v_{∞} from Prinja et al. (1990); Howarth et al. (1997); $v \sin i$ from Howarth et al. (1997) but see also Penny (1996). (c) $v \sin i$ from Uesugi & Fukuda (1982). (α) CPD-59 $^{\circ}$ 2603 is probably a multicomponent and only parameters for component A (Howarth et al. 1997) are indicated here.

TABLE 2
OBSERVATIONS OF STARS IN THE MAGELLANIC CLOUDS^a

Star	Sp. Type Reference	l ($^{\circ}$)	b ($^{\circ}$)	V $E(B-V)$ (mag.)	v_{∞} (km s^{-1})	Δt^b (day)	UT-Date	Rootname	Remarks ^c
Sk $-67^{\circ}167$	O4 Inf ⁺ W95	277.87	-32.47	12.54 0.14	2005 ^b	285	1999-12-17 2000-09-27	P1171902 P1171901	
Sk $-71^{\circ}45$	O4-5 IIIf W77	281.86	-32.03	11.47 0.20	2500 ^c	2.7 1.0 0.5	2000-10-02 2000-10-05 2000-10-06	P1031501 P1031503 P1031502	
Sk $-67^{\circ}111$	O6 Ia(n)fp var W02	277.75	-32.97	12.57 0.11	2090 ^d	138	1999-09-26 2000-10-20	X0200101 P1173001	RV var?
BI 208	O7 Vz Wpc	277.54	-32.30	14.02 0.03	...	0.5 0.1 1.2	2000-09-30 2000-10-01 2000-10-01	P1172704 P1172703 P1172702	
BI 272	O7 III-II: Wpc	277.24	-31.32	13.20 0.17	3400 ^c	287	1999-12-18 2000-09-29	P1172902 P1172901	
Sk $-67^{\circ}101$	O8 II((f)) W02	277.78	-33.05	12.63	2005 ^b	284	1999-12-20 2000-09-29	P1173403 P1173401	
BI 173	O8 II: W02	279.67	-32.68	13.00 0.17	2850 ^c	61.9	2000-10-03 2000-12-04	P1173201 P1173202	RV var
Sk $-67^{\circ}191$	O8 V C86	277.66	-32.33	13.46 0.10	1750 ^b	287	1999-12-17 2000-09-29	P1173102 P1173101	
Sk $-68^{\circ}03$	O9 I C86	279.70	-35.93	13.13 0.48	...	1.3	2000-10-04 2000-10-05	A0490402 A0490401	
Sk $-69^{\circ}124$	O9 Ib: Wpc	279.61	-32.86	12.66 0.12	1430 ^b	62.1	2000-10-03 2000-12-04	P1173601 P1173602	
Sk $-65^{\circ}44$	O9 V C86	277.78	-33.05	12.63 0.14	...	140	2001-10-27 2002-03-16	P1173401 P1173401	
Sk $-67^{\circ}05$	O9.7 Ib F88	278.89	-36.32	11.34 0.15	1665 ^d	2.8	2000-10-04 2000-10-07	P1030704 P1030703	
Sk $-65^{\circ}21$	O9.7 Iab W95	276.19	-35.79	12.02 0.20	1330 ^d	0.6 0.1 0.4	2000-10-05 2000-10-05 2000-10-05	P1030901 P1030904 P1030903	
Sk $-71^{\circ}08$	O9 II C86	282.52	-33.88	13.25 0.08	...	636	1999-12-21 2001-09-17	A0491401 A0491402	
Sk $-70^{\circ}85$	B0 I J01	281.26	-33.31	12.30 0.15	...	636	1999-12-21 2001-09-17	A0491301 A0491302	
Sk $-68^{\circ}41$	B0.5 Ia F91	279.02	-34.82	12.01 0.16	865 ^b	290	1999-12-18 2000-10-03	P1174102 P1174101	
AV 488	B0.5 Iaw W95	300.51	-43.66	11.90 0.14	1040 ^b	0.1 2.0	2000-10-08 2000-10-08 2000-10-10	P1176803 P1176802 P1176801	
Sk $-67^{\circ}28$	B0.7 Ia F88	278.06	-35.69	12.28 0.10	...	4.1	1999-12-16 1999-12-20	A0490201 A0490202	
Sk $-68^{\circ}75$	B1 I J01	278.65	-33.17	12.03 0.19	...	6.5	2000-10-03 2000-10-10	A0490501 A0490502	
Sk $-70^{\circ}120$	B1 Ia F88	280.72	-30.47	11.59 0.14	...	0.1	2000-09-28 2000-09-28	A0491002 A0491001	
Sk $-67^{\circ}14$	B1.5 Ia F91	278.27	-36.05	11.52 0.10	610 ^b	4.3 0.6	2000-09-27 2000-10-01	P1174201 P1174203	
AV 18	B2 Ia L97	303.36	-44.02	12.48 0.21	...	381	2000-10-02 2000-05-29 2001-06-13	P1174202 A1180101 B0890101	

^aAV 18 and AV 488 are SMC stars, all the others are LMC stars.

^b Δt between successive observations.

^cRadial velocity variation detected or suspected.

References. — (a) Sources of spectral type: C86=Conti et al. (1986); F88, F91=Fitzpatrick (1988, 1991); J01=Jaxon et al. (2001); L97=Lennon (1997); W77, W95, W02=Walborn (1977); Walborn et al. (1995, 2002); Wpc=Walborn (private communication, 2001). v_{∞} from (b) Prinja & Crowther (1998), (c) Massa et al. (2003), (d) Patriarchi & Perinotto (1992), see also Bianchi et al. (2000, 1800 km s^{-1}) for Sk $-67^{\circ}111$.

TABLE 3
CHARACTERISTICS OF WIND PROFILE VARIABILITY IN O VI, S IV, AND P V ^a

Star	Sp. Type	O VI	S IV	P V
MW sample				
HDE 303308	O3 V((f))	v. [1100, 2700]	n.v.	n.v.
HD 64568	O3 V((f*))	n.v.	n.v.	n.v.
CPD-59°2600	O6 V((f))	v.(n)	n.v.	n.v.
CPD-59°2603	O7 V	v. [1500, 2350]	n.v.	n.v.
HD 152590	O7.5 V	v. [1100, 1900]	n.v.	n.v.
HD 61347	O9 Ib	v. [900, 1900]	v. [200, 1600]	n.v. (n)
HD 210809	O9 Iab	v. [700, 2200]	v. [300, 2200]	v. [300, 2200]
HD 153426	O9 II	n.v.(n)	n.v.	n.v.
HD 91651	O9 V:n	n.v.	n.v.	n.v.
HD 92554	O9.5 II:n	v. [800, 1400]	v. [700, 1300]	n.v. (n)
HD 168941	O9.5 II-III	v. [1000, 2100]	n.v.	n.v.
HD 156292	O9.5 III	n.v.	n.v.	n.v.
HD 163892	O9 IV ((n))	v. [950, 1550]	n.v.	n.v.
HDE 308813	O9.5 V	n.v.	n.v.	n.v.
HD 186994	B0.2 IV	n.v.	n.v.	n.v.
CPD-72°1184	B0 III	n.v.	n.v.	n.v.
HD 192035	B0 III-IV(n)	v. [800, 1050]	n.v.	n.v.
HD 47417	B0 IV	v. [650, 1025]	n.v.	n.v.
HD 203374A	B0 IVpe	n.v.	n.v.	n.v.
BD +53°2820	B0 IVn	n.v.	n.v.	n.v.
HD 191495	B0 IV-V	v.(n)	n.v.	n.v.
HD 195965	B0 V	n.v.	n.v.	n.v.
HD 207538	B0.2 V	n.v.	n.v.	n.v.
HD 187459	B0.5 Ib	v. [750, 1550]	v. [750, 1550]	v. [750, 1550]
HD 224151	B0.5 II	v. [400, 1100]	n.v.	n.v.
HDE 332407	B0.5 III:	v.(n)	n.v.	n.v.
HD 161807	B0.5 III:n	v. [975, 1200]	n.v.	n.v.
HD 172140	B0.5 III	v. [1000, 1400]	n.v.	n.v.
HD 62866	B0.5 III:n	v. [800, 1150]	n.v.	n.v.
HD 97913	B0.5 IVn	v. [1200, 1650]	n.v.	n.v.
BD +35°4258	B0.5 Vn	v. [600, 950]	n.v.	n.v.
HD 148422	B1 Ia	v.(n)	n.v.	n.v.
HD 191877	B1 Ib	v.(n)	n.v.	n.v.
HDE 235783	B1 Ib	v.(n)	n.v.	n.v.
BD +48°3437	B1 Iab	n.v.	n.v.	n.v.
HD 225757	B1 III:n	n.v.	n.v.	n.v.
HD 91597	B1 III:ne	v. [900, 1900]	n.v.	n.v.
BD +52°3210	B1 V	n.v.	n.v.	n.v.
HD 73	B1.5 IV	n.v.(n)	n.v.	n.v.
HD 202347	B1.5 V	n.v.	n.v.	n.v.
BD +53°2885	B2 III	n.v.	n.v.	n.v.
HD 47961	B2 V	n.v.	n.v.	n.v.
HD 51013	B3 V	n.v.	n.v.	n.v.
HD 47777	B3 V	n.v.	n.v.	n.v.
MC sample				
Sk-67°167	O4 In ⁺	n.v.	n.v.	n.v.
Sk-71°45	O4-5 III:f	v.(n)	n.v.	n.v.
Sk-67°111	O6: Iafpe	v.	v. [500, 1600]	v. [500, 1600]
BI 208	O7 Vz	v. [800, 1900]	n.v.	n.v.
BI 272	O7: III-II:	v. [400, 2600]	n.v.	n.v.
Sk-67°101	O8 II((f))	v. [1300, 1525]	n.v.	n.v.
BI 173	O8 II:	v.	n.v.	n.v.
Sk-67°191	O8 V	v. [1150, 1900]	n.v.	n.v.
Sk-68°03	O9 I	n.v.	n.v.	n.v.
Sk-69°124	O9 Ib:	v. [600, 1600]	v.(n)	n.v.
Sk-65°44	O9 V	v. [1200, 1600]	n.v.	n.v.
Sk-67°05	O9.7 Ib	v.	v.	n.v.
Sk-65°21	O9.7 Iab	v.	v.	n.v.
Sk-71°08	O9 II	n.v.	n.v.	n.v.
Sk-68°41	B0.5 Ia	v. [100, 1200]	v. [100, 1200]	n.v.
AV 488	B0.5 Iaw	n.v.	n.v.	n.v.
Sk-67°28	B0.7 Ia	n.v.	n.v.	n.v.
Sk-70°85	B0 I	v.	v. [100, 1200]	n.v.
Sk-68°75	B1 I	n.v.	n.v.	n.v.
Sk-70°120	B1 Ia	n.v.	n.v.	n.v.
Sk-67°14	B1.5 Ia	n.v.	n.v.	n.v.
AV 18	B2 Ia	n.v.	n.v.	n.v.

^av.: wind variable; n.v.: wind not variable; (n)=noisy. The approximate range of the profile variation is given in square brackets. The values are expressed in km s^{-1} and should be multiplied by -1 . For the Magellanic stars, this range can be more uncertain because of possible overlapping of the O VI profiles; and in cases where it is completely uncertain, we do not indicate any values.

TABLE 4
O VI WIND ABSORPTION

Star	Sp. Type	v_{∞} (km s ⁻¹)	v_{abs} (km s ⁻¹)	Strength
MW sample				
HD 152590	O7.5 V	1785	1700 ^a 1300	strong weak
HD 61347	O9 Ib	1775	1250	weak
HD 153426	O9 II	2200	2150	strong
HD 92554	O9.5 II _n	1260	1125	strong
HD 168941	O9.5 II-III	1795	1625 ^a 1250	strong weak
HD 156292	O9.5 III	1355	1300 1100	strong weak
HD 163892	O9 IV ((n))	1405	1320 1175	medium medium
CPD-72°1184	B0 III	...	1075	medium
BD +53°2820	B0 IV _n	...	1200	medium
HD 187459	B0.5 Ib	1185	1125	strong
HD 224151	B0.5 II	1280	1250	strong
HDE 332407	B0.5 III:	...	1275	medium
HD 161807	B0.5 III:n	...	1120	weak
HD 62866	B0.5 III _n	...	980 1130	weak weak
HD 191877	B1 Ib	...	1000	strong
HD 91597	B1 III _{ne}	...	1170 1370	weak weak
MC sample				
Sk -67°101	O8 II((f))	2005	950	weak
Sk -67°191	O8 V	1750	1700 ^a	strong
Sk -69°124	O9 Ib:	1430	1150 1350	medium medium
Sk -67°05	O9.7 Ib	1665	1000	strong
Sk -65°21	O9.7 Iab	1330	1000	medium
Sk -70°85	B0 I	...	850	strong
Sk -68°41	B0.5 Ia	865	800	strong

Note. — v_{abs} corresponds to the deepest part of the O VI wind absorption feature. The strength corresponds to the strength of the O VI $\lambda 1038$ wind absorption feature, see § 4 for more details. (a) The O VI $\lambda 1038$ wind absorption feature is blended with the interstellar O VI $\lambda 1032$, but the latter is too wide and strong to be entirely interstellar.